How far can we trust forestry estimates from low-density LiDAR acquisitions? The Cutfoot Sioux experimental forest (MN, USA) case study

Published version:

DOI:10.1080/01431161.2020.1723173

(Article begins on next page)

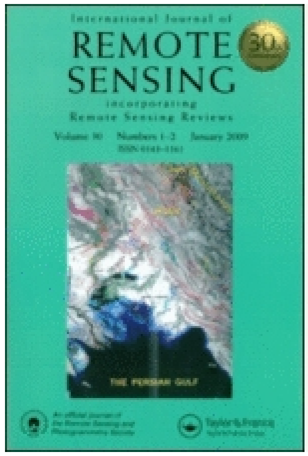

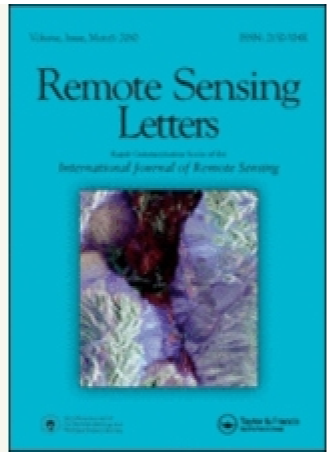

How far can We trust Forestry Estimates from Low Density LiDAR Acquisitions? The Cutfoot Sioux Experimental Forest (MN, USA) Case Study

Journal:	*International Journal of Remote Sensing*
Manuscript ID	TRES-PAP-2019-0377.R1
Manuscript Type:	IJRS Research Paper
Date Submitted by the Author:	04-Oct-2019
Complete List of Authors:	Borgogno Mondino, Enrico; Universita degli Studi di Torino Dipartimento di Scienze Agrarie Forestali e Alimentari Fissore, Vanina; Universita degli Studi di Torino Dipartimento di Scienze Agrarie Forestali e Alimentari Falkowski, Michael; Colorado State University College of Agricultural Sciences Palik, Brian; USDA Forest Service, Northern Research Station
Keywords:	Airborne laser scanning (ALS), data analysis, Tree mapping
Keywords (user defined):	Bias modeling, Error analysis, Data reliability

How far can We trust Forestry Estimates from Low Density LiDAR Acquisitions? The Cutfoot Sioux Experimental Forest (MN, USA) Case Study

Enrico Borgogno Mondino[1], Vanina Fissore[1*], Michael J. Falkowski[2], Brian Palik[3]

[1]*DISAFA, University of Torino, L. go Paolo Braccini 2, 10095, Grugliasco (TO), Italy;*
e-mails: enrico.borgogno@unito.it; vanina.polito@gmail.com.
[2]*Colorado State University, Fort Collins, Colorado 80523, USA;*
e-mail: M.Falkowski@colostate.edu.
[3]*USDA Forest Service, Northern Research Station, 1831 Hwy. 169. E. Grand Rapids, MN 55744, USA;*
e-mail: bpalik@fs.fed.us

**Corresponding author*

How far can We trust Forestry Estimates from Low Density LiDAR Acquisitions? The Cutfoot Sioux Experimental Forest (MN, USA) Case Study

Abstract

Aerial discrete return LiDAR technology (ALS – *Aerial Laser Scanner*) is nowadays widely used for forest characterization due to its high accuracy in measuring vertical and horizontal forest structure. Random and systematic errors can occur and affect the native point cloud, ultimately degrading ALS data accuracy, especially when adopting datasets that were not natively designed for forest applications; a detailed understanding of how uncertainty of ALS dataset could affect accuracy of derivable forest metrics (e.g. tree height, stem diameter, basal area) is, in this case, required, looking for eventual error biases that can be possibly modelled to improve final accuracy. In this work a low-density ALS dataset, originally acquired by the State of Minnesota (USA) for non-forestry related purposes (i.e., topographic mapping) was processed attempting to characterize forest inventory parameters of the Cutfoot Sioux Experimental Forest (north-central Minnesota, USA). Since accuracy of estimates strictly depends on the applied species-specific dendrometric models a first required step was to map tree species all over the forest. A rough classification, aiming at separating conifers from broadleaves, was achieved by processing a Landsat 8 OLI scene. ALS-derived forest metrics initially showed to greatly overestimate those measured at the ground in 230 plots. Oppositely, ALS-derived tree density was greatly underestimated, placing less trees in the area. Aiming at reducing ALS measures uncertainty, trees belonging to the dominated plane were removed from the ground dataset, assuming that they could not properly be detected by low density ALS measures. Consequently, MAE (*Mean*

Absolute Error) values significantly decreased to 4.0 m for tree height and to 0.19 cm for diameter estimates. Remaining discrepancies were proved to be related to a *bias* affecting the native ALS point cloud, that was modelled and removed. MAE values finally resulted 1.32 m for tree height, 0.08 m for diameter, 8.5 m^2/ha for Basal Area, and 0.06 m for Quadratic Mean Diameter. Specifically focusing on tree height and diameter estimates, significance of differences between ground and ALS estimates was tested in respect of the expected "best accuracy", whose definition is given in the text. Results showed that after correction: 94.35% of tree height differences were lower than the correspondent reference value (2.86 m); 70 % of tree diameter differences were lower than the correspondent reference value (4.5 cm for conifers and 6.8 cm for broadleaves). Finally forest parameters were computed for the whole Cutfoot Sioux Experimental Forest.

Main findings of this work are: first, all forest estimates based on low density ALS point cloud can be reasonably given only at plot level and not at tree level; second, tree height estimates obtained by low density ALS point clouds at plot level are highly satisfying only after testing and modelling eventual error bias, while, on the contrary, diameter, basal area and QMD estimates majorly suffer from uncertainty making desirable a higher point density and, probably, a better mapping of tree species (wherever possible) than the one that a remote sensing based one can generate.

Keywords: low density ALS, forest parameters estimate, accuracy assessment, LiDAR measures bias modelling.

Introduction

Discrete return LiDAR technology from aircraft (ALS) is a proven tool for many forest applications. Due to its high accuracy in measuring vertical and horizontal forest structure, ALS for forest characterization has increased considerably over the last few decades. It has been successfully applied in support of operational forest inventories by deriving accurate, high resolution estimates of many forest structural properties including tree height (Morsdorf et al., 2004; Andersen et al., 2006; Hopkinson et al., 2004; Edson and Wing, 2011; Saremi et al., 2014; Falkowski et al., 2006; 2008), diameter (Popescu, 2007; Saremi et al., 2014), canopy size (Means et al., 2000; Popescu and Zhao, 2008), volume (Hinsley et al., 2002; Riaño et al., 2004; Latifi et al., 2015) and vertical distribution of tree canopy (Dubayah and Drake, 2000). In traditional forest inventories, trees attributes are collected in discrete ground sample plots, which are assumed as representative of the whole forest. Conversely, ALS data can provide information across large spatial extents, ranging from tree to landscape scales (McRoberts et al., 2010). ALS-derived tree heights can be used to estimate forest structural parameters such as tree diameter and basal area via numerical model estimation, both at the species or mixed-species level, that relate height to other features (e.g tree diameter; VanderSchaaf, 2012). Therefore, a detailed understanding of how uncertainty in the LiDAR dataset affects the uncertainty of derived forest inventory metrics, i.e. tree height, stem diameter, and basal area, is required.

A specific focus has to be done on the opportunity related to the use of low density LiDAR acquisitions or of ALS datasets acquired for different purposes than forestry applications. In fact, nowadays many public institutions make accessible for free low density LiDAR acquisitions acquired few years ago often aimed at topographic representation. These freely available datasets often cover nation-wide areas and represent an opportunity in the field of forest research. In last years, low-density LiDAR dataset have been already used, for example to investigate its utility in estimating forest aboveground biomass in the mountainous forests of norther Italy (Montagnoli A. et al., 2015) or for testing tree species identification (e.g. Suratno A. et al., 2009).

With specific focus on the present work, a free low-density ALS dataset, acquired by the State of Minnesota (USA), was used together with Landsat 8 OLI (*Operational Land Imager)* data to characterize the forest structure of the Cutfoot Sioux Experimental Forest (CEF) located in north-central Minnesota (USA). The joint use of ALS data with multispectral satellite data has been adopted since ALS measures cannot be efficiently used to separate tree species, while multispectral satellite data, in spite of its reduced geometric resolution, can differently achieve this task in mapping main vegetation classes (e.g. broadleaved trees versus coniferous trees) based on their spectral signatures. Indeed, determining tree species class is of paramount importance when using tree height as predictor of other tree parameters via numerical dendrometric models.

Specifically, structural properties of forest, were investigated at both tree and plot scale; in particular, at tree-scale the following measures were considered: *a*) tree height (m) and *b*) tree diameter (m). At the plot-scale: *a*) tree density; *b*) plot mean height (m); *c*) plot mean diameter (m); *d*) plot mean basal area (BA, m^2/ha)) and *e*) Quadratic Mean Diameter (QMD, cm).

Main explored hypotheses were, first, to assess if low density LiDAR derived forest estimates could be given at tree level and/or at plot level, and, second, if low density LiDAR derived estimates were reliable if compared to the same obtained from ground data collection. To test these hypotheses, the above listed forest parameters were computed from both ground and ALS data and their consistency tested at both tree- and plot-scale. A rather weak consistency was initially found. Authors hypothesized that this not favorable situation could be due to two factors; first, a limitation of the system, as it is a "low-density" acquisition system, and, second, a possible error *bias* affecting the native point cloud. In fact, it is known that LiDAR raw data can be affected by many random and systematic errors introduced during data acquisition (depending from flight acquisition geometry) [Coveney, 2013] data processing, and depending on the nature of the surface hit by the laser pulse (e.g. land cover categories, vegetation classes, slope) [Hyyppä et al., 2005]. Consequently, a further investigation was achieved and some actions, included error bias modelling, adopted to correct ALS estimates, at both tree and plot scale. We finally computed forest inventory parameters for the whole study area at the plot-scale. Measures distribution was summarized computing correspondent Empirical Cumulative Distribution Functions (ECDF).

Materials and Methods

Study area

The study area is the Cutfoot Experimental Forest (CEF, 507 hectares) located within the Chippewa National Forest in north-central Minnesota (Itasca county, USA) at 47°40′ N, 94°5′ W (figure 1). CEF is dominated by red pine (*Pinus resinosa* Ait.) that originated after fires that occurred between 1864 and 1918 (Adams et al., 2004). Additional species include jack pine (*Pinus banksiana* Lamb.) and eastern white pine (*Pinus strobus L.*), paper birch (*Betula papyrifera* Marsh.) and quaking Aspen (*Populus tremuloides* Michx.).

CEF is nearly equally divided in: about 273 ha that have had a range of forest management activities, including both traditional commercial timber harvests (CEF cut and sold reports, USFS Grand Rapids, MN) and numerous silvicultural experiments

(Buckman, 1964; Adams et al., 2004; Bradford and Palik, 2009; D'Amato et al., 2010); about 234 ha occupied by the Sunken Lake Natural Area, with is largely old-growth forest (Aakala et al., 2012; Fraver and Palik, 2012).

[FIGURE 1]

Ground data

Ground data were collected as part of a forest-wide survey between May and August 2013 within 230 semi-permanent forest inventory plots: 130 located in the managed area and 100 located in the Sunken Lake Natural Area. Surveyed trees totaled 9851, with an average of about 43 trees per plot. Sampling plots had a nested design comprised of three circular plots: in the outer plot, which had a radius of 16 m, tree species were identified and diameters measured for all trees ≥ 19.3 cm diameter at breast height (DBH). The central plot, which had a radius of 11.3 m, was used to tally trees ≥ 8.9 cm and < 19.3 cm DBH. Lastly, the innermost plot, which had a radius of 3.5 m, was used to tally trees with DBH < 8.9 cm and height > 0.30 m. This field sampling design is a standard approach for forest vegetation measurements in the study area. We used the result ground data because it was freely available for use and because it was collected near in time to the LiDAR data (see next section).

While diameters were directly measured at tree level, other forest parameters were derived by computation using appropriate species-specific regression models calibrated on the US FIA (*Forest Service Forest Inventory and Analysis*) database of Minnesota. Single tree measures and estimations were then averaged at plot-level to derive mean height, mean diameter, mean basal area (BA) and quadratic mean diameter (QMD) for each plot.

During ground data collection, the position of each plot centre was georeferenced by GNSS (Global Navigation Satellite System) by a GPSMAP® 60CSx, providing a position accuracy of about 10 m. Individual tree position was measured as distance (m) and azimuth (degrees) from the plot center. During data processing, tree positions within the plot were recovered moving from plot center according to distance and azimuth values.

Remotely sensed data

ALS raw data were freely obtained from the Minnesota Geospatial Information Office website (MnGeo, http://www.mngeo.state.mn.us) for the Central Lakes Region of MN. The dataset was collected over Itasca County, MN in April 2012. The data were provided in the UTM NAD83 Zone 15N coordinate system. Vertical and horizontal accuracy values were 0.5 m and 1.15 m, respectively, at a 95 percent confidence level, and flight lines side overlap was 25%. ALS60, ALS70 and Optech ALTM Gemini systems were used for data acquisition. General specifications of acquisition conditions included the following: AGL (*Above Ground Level*) average flying height ranged between 2072.6 m and 2377.4 m; MSL (*Mean Sea Level*) average flying height ranged between 2712.7 m and 2766.0 m; Average Ground Speed was about 277 km/h; Field of View (FOV) was 40 degrees; LiDAR pulse rate ranged between 99 kHz and 115.3 kHz and the scan rate between 25.1 Hz and 38 Hz. Multiple returns were recorded up to 5 returns; intensity values were recorded @8-bit quantization. Pulse returns density was of 0.78 pls/m^2. The raw point cloud was processed via LASTools (Rapidlasso GmbH) to generate gridded digital surface model (DSM) and digital terrain model (DTM) with a 1 m cell size. A canopy height model (CHM) was generated by differencing the DSM and DTM and a *local maxima* algorithm was run to map potential trees from the correspondent CHM using SAGA GIS 7.2.

A Level 2 Landsat 8 OLI (*Operational Land Imager*) multispectral image, acquired on 11th November 2013, was downloaded from the EarthExplorer distribution system (http://www.earthexplorer.usgs.gov). It was supplied already calibrated in at-the-ground reflectance. A Landsat-8 OLI image was adopted because its geometric resolution of 30 m is consistent with ground plots size (16 m radius). In this way, each forest plot can be assumed as corresponding to a Landsat pixel and, therefore, be comparable. Moreover, being Lansat-8 OLI multispectral, it permitted to use spectral signatures of conifers and broadleaves to classify the entire forest.

A caveat regarding the LiDAR data and ground truth data is that were collected more than one year apart. However, the ground data is specifically based on measurements on trees; short of changes caused by catastrophic events (or which there were none in the study area during the period of record), there would be virtually no detectable differences in measurements taken in spring 2012 versus summer 2013. Any difference in diameter, height, or basal area would be within the range of measurement error. Moreover, ground data was used only to directly provide diameters and trees location, and consequently the effect of the season (LiDAR: April 2012 vs Ground data: summer 2013) is inconsequential. Moreover, LiDAR acquisition for the study was collected in April, which is the beginning of a leaf-on season in the study area and the forest is conifer dominated, so the influence of differences in time of acquisition between ground and LiDAR data was minimized.

Data analysis

It is worth pointing out that ALS-derived and ground measures follow opposite paradigms when generating tree-level forest inventory measures. For example, traditional forest inventory approaches typically use tree diameter measurements to model tree height and other inventory parameters, whereas ALS-based approaches use tree height measurements to retrieve diameter and other inventory parameters. Both approaches operate through numerical models that relate diameter with height. If we test consistency between tree diameters, the ones from LiDAR are "indirectly" derived by numerical modelling from heights; if we test consistency between heights, the ones from ground are those generated by numerical approaches. Therefore, we have to preventively define some reference values ("best reachable accuracy") to compare uncertainty with. These can be defined while calibrating local numerical model relating diameters and height (or vice versa) by an Ordinary Least Squares (OLS) approach. A flowchart showing overall phases of achieved analysis is available in the Supplemental (Figure 2).

Ground Data Processing

Using ground sampled tree diameters, we estimated, by OLS the coefficients of the following numerical dendrometric model relating tree height to its diameter (Perala and Alban, 1993).

$$H_s = a_s D^{b_s} + \varepsilon_s \qquad (1)$$

where H_s is the estimated height for a specific species, *D* the ground sampled diameter, a_s and b_s are species-specific coefficients and ε_s the estimated model uncertainty.

Model was calibrated using the dataset from the US FIA (*Forest Service Forest Inventory and Analysis*) database for Minnesota, downloaded from the FIA database website (version 4.0, Woudenberg et al. 2010, US Forest Service, 2011). Only the most frequently occurring species in CEF plots were considered. For the conifer class (hereinafter called "C"): balsam fir, eastern white pine, jack pine and red pine were adopted; for the broadleaf class (hereinafter called "B"): paper birch, quaking aspen and northern red oak. Calibrated models were then used to compute tree heights within the surveyed plots in CEF.

The US FIA data for Minnesota was chosen because the calibration of the regression models required a large amount of (freely available) inventory data to be as reliable as possible, and, moreover, it needed to be specific for the species present in the study area, which was not obtainable from any other source.

To make all diameter classes equally represented during model calibration, OLS estimation was achieved by relating diameter and height average values of predefined classes. These were defined splitting the diameter range of variation into classes of a width of 2.5 cm and looking for the correspondent height values. Class diameter and height values were averaged and model parameters estimated accordingly. Standard deviation of heights belonging to the class was computed as well. The mean value of all class standard deviations ($\sigma^H{}_m$) was assumed as reference "best" uncertainty to compare ALS-derived height with. In other words, height estimations from the model were assumed to represent a class of heights having an internal variability equal to $\sigma^H{}_m$. All computation concerning model calibration were run through in-house appositely developed IDL (*Interactive Data Language*) routines.

Trees basal area (g_i) was computed according to eq. 2:

$$g_i = \frac{\pi}{4} \cdot d_i^2 \qquad (\mathrm{m}^2) \qquad (2)$$

where d_i^2 is the tree diameter.

Estimated single tree measures were then averaged at plot level. For each plot, mean diameter ($D^G{}_\mu$) and mean height ($H^G{}_\mu$) were computed. Plots total basal area (BA^G) was considered and computed by eq. 3, including all species in plot:

$$BA = \frac{\sum_{i=1}^{n} g_i}{A_p} \quad (m^2/ha) \qquad (3)$$

where g_i is the same of eq. 2, n is the number of surveyed trees in each plot and A_p the area (ha) of the plot.

Moreover, plots mean tree density ($T^G{}_{pha}$) and plot quadratic mean diameter (QMD^G) were computed respectively according to eq. 4 and 5.

$$T^G{}_{pha} = \frac{n.\ tree}{A_p} \quad (n.\ trees/ha) \qquad (4)$$

$$QMD^G = \frac{BA/T_{pha}}{0.00007854} \quad (cm) \qquad (5)$$

To summarize data at plot level single tree diameters and heights were averaged within the plot.

Mapping Tree Species by Satellite Imagery

Accuracy of estimates strictly depends on the possibility of applying the appropriate dendrometric model to the proper tree species. Since no a-priori knowledge of vegetation type was given, a preliminary step was needed to classify tree species before models could be applied. From an operational point of view, at-species level classification of forest (tree by tree) was not possible. Nevertheless, a rougher classification, aiming at separating conifers from broadleaves, was achieved processing multispectral imagery.

To properly approach image classification, main tree species of CEF (table 1), were analysed at plot level; depending on the proportion of conifer and broadleaves, plots were labelled as “C” if they were ≥ 70% coniferous species or “B” if they were ≥ 70% broadleaves species. Mixed plots were excluded from the analysis. Fifty-four plots were labelled as “B” = broadleaves, 97 as “C” and 79 were not considered for classification training, being populated by mixed vegetation. Excluded plots did not enter any of the following computations. It is worth to highlight that geometric resolution of Landsat

OLI images (30 m) is consistent with plot size (16 m radius). Consequently, one can assume that each forest plot corresponds to a Landsat pixel. To collect an adequate number of training pixels each plot was used as starting point to define the correspondent Region of Interest (ROI), that was obtained by region growing looking for similar pixels around the selected one. Any eventual relative positioning error between ground and ALS measures in respect of Landsat imagery can be neglected, being certainly lower and lower if compared with Landsat pixel size. A supervised classification (*Minimum Distance* algorithm; Richards, 1999) was therefore run to generated the correspondent classification map that was validated by confusion matrix.

ALS Data Processing

LiDAR point cloud was processed by LASTools libraries. The following operations were performed: a) point returns presenting a scanning angle greater than 15 degrees were filtered out (accuracy reduces when scanning angles are higher than 12-14 degrees over dense forest stands; Gatziolis & Andersen, 2008); b) points were classified into "ground" and "not-ground" by LASTools "*lasground*" library (natural context parameters); c) regularization of points cloud was achieved by *las2dem* tool obtaining the correspondent DTM and DSM with a pixel size of 1 m.

A CHM of the area was generated by differencing of DSM and DTM. A specifically designed *local maxima* filter was run over CHM, to detect pixels which likely represented the top of trees.

Tree height from ALS was extracted from CHM at the locations of the detected *local maxima*. Tree diameter was estimated by eq. 6 that proved to well approximate experimental data. Model type was specifically selected and used by authors with no concern about pre-existing references from literature, but in consequence of appositely performed test involving available data.

$$D_t = e^{a_t} \cdot H^{b_t} + \varepsilon_t \tag{6}$$

where a_t and b_t are <u>tree-species dependent</u> coefficients and ε_s is the estimated model uncertainty for D_t. Differently from ground measures, ALS estimates of D_t were computed by eq. 6, differently calibrated in respect of “C” and “B” macro-classes. This was obtained including associated tree species according to table 1.

To make all height values equally represented during model calibration, OLS estimation was achieved relating height and diameter mean values of predefined aggregated classes from the native measures. Height classes were defined with a width of 25 cm; included measures, together with the correspondent diametric ones, were consequently averaged at class level. The dendrometric model of eq. 6 was therefore calibrated in respect of the averaged diameter and height class values. Standard deviation of each diameter class was computed too. Unlike direct dendrometric models (eq. 1), the mean of the standard deviations of class diameter was lower than the correspondent MAE^D (Mean Absolute Error, Willmott & Matsuura, 2005)~~.~~ MAE^D was therefore assumed as reference “best” accuracy in diameter estimation from ALS data.

Forest class map from Landsat 8 imagery (FCM) was used to assign the appropriate tree class to each ALS detected tree, making possible the application, at tree level, of the right dendrometric model (eq. 6).

Once height and diameter were estimated for each detected tree, T^L_{pha}, D^L_{μ}, H^L_{μ}, BA^L, and QMD^L were computed for each plot by averaging.

According to FCM (“C” and “B” classes), forest parameters were finally computed for the whole CEF study area at plot level, generating the correspondent raster maps (cell size = 30 m) of the estimates of forest parameters.

Ground vs ALS: testing consistency of measures

To compare measures, we firstly tested consistency of tree positions as detected from ALS by the *Local Maxima* algorithm with the one surveyed during field campaign, showing a significant displacement. Consequently, a tree-to-tree comparison was retained unreasonable and comparisons operated at plot level. Consequently, estimates from ALS were computed at-tree level, but comparisons with ground data were operated by aggregating measures. A first comparison involving all the detected trees in respect of the surveyed ones was achieved by computing ECDFs of T_{pha}, H_{μ}, D_{μ}, *BA,* and *QMD* for both ground and LAS measures/estimates.

Due to the importance of height measures in many forest parameters computations, and to the current trend of using LAS data for its determination a first comparison was achieved with reference to plots average tree height values (H^{G}_{μ} and H^{L}_{μ}). Uncertainty of T^{L}_{pha}, D^{L}_{μ}, H^{L}_{μ}, BA^{L}, and QMD^{L} , was measured as MAE (eq. 7).

$$MAE = \frac{1}{n}\sum_{i=1}^{n}|f_i - y_i| \tag{7}$$

where f_i is the predicted (ALS) value, y_i is the ground correspondent value and *n* the number of observations (n. plots).

Initially we considered that such big differences could be related to the underestimation of trees number by ALS, that, necessarily, may not completely describe vegetation under the main canopy cover (Reitberger J., et al., 2009). This in particular affected aggregated forest parameters (BA, QMD, T_{pha}) strictly depending on tree number. To test this hypothesis we sorted, for each plot, ground surveyed trees according to their height, selecting the tallest ones in number equal to those detected by ALS. We assumed that this operation removed from analysis the trees of the dominant layers that were not recorded by LiDAR, making observation distributions more similar. New ground tree height values were then calculated and compared with the ALS-derived ones. Since comparison still showed dissimilarities, we tested if a *bias* could affect the native point cloud. For this, we compared ALS estimates with the “filtered/reduced” ground surveyed ones. *Bias* was tested only for tree heights. We related $\Delta H_\mu = H^L{}_\mu$ - $H^G{}_\mu$ with $H^L{}_\mu$ by scatterplot, finding a strong correlation, that was modelled to correct LAS measured tree heights both at plot and tree level. This operation proved to reduce estimates uncertainty.

After quantification of tree height accuracy (MAE was computed at plot level) affecting “corrected” ALS-derived estimates, significance of both ΔH_μ and $\Delta D_\mu = D^L{}_\mu - D^G{}_\mu$ was tested. Only $|\Delta H_\mu|$ and $|\Delta D_\mu|$ higher than expected “best” accuracy ($\sigma^H{}_m$, MAE^D respectively for tree height and diameter estimates) were assumed as significant. To test this condition the ECDFs of ΔH_μ and ΔD_μ from LIDAR, both from “*biased*” and “*unbiased*” measures, were computed for the whole CEF. These were compared to ground estimates, demonstrating that few field surveyed measures can well represent the most of the forest they belong too.

Finally, a comprehensive description of CEF using all forest parameters was developed and interpreted. Flowchart relative to error quantification and modelling, and to ECDF comparison analysis is available in Supplemental (Figure 3).

Results and Discussions

Ground Data Processing

The dendrometric model of eq. 1 was calibrated by OLS for the main tree species surveyed in CEF. Table 1 reports estimated coefficients and the following statistics: model MAE (tree height estimate accuracy); R, Pearson’s correlation coefficient between observations and estimates; $\sigma^H{}_{species}$, mean standard deviation of height class for each considered tree species.

Values of table 1 were averaged over all the species making possible to somehow synthesize mean accuracy expectations. The mean values were found to be 1.39 m and 2.86 m respectively for MAE^H and $\sigma^H{}_m$. Since the latter was the highest, it was assumed as "best expectable accuracy" for tree height measurements. In other words, no tree height estimates from other sources is expected to be more accurate than the average intra-species variability, represented by $\sigma^H{}_m$.

[TABLE 1]

Calibrated dendrometric models were consequently, and accordingly, applied to all ground surveyed trees to give height estimates. Single trees height and diameter were, then, averaged over the plot and correspondent BA and QMD calculated. Moreover, at-plot-level computed forest parameters were averaged over the previously defined macro-classed ("B" = Broadleaves and "C" = Conifers) considering that plots were preventively assigned to "B" or "C" . At-class-level averaged forest parameter values will be hereinafter indicated as: $D^G{}_\mu$, $H^G{}_\mu$, BA^G, $T^G{}_{pha}$, and QMD^G . Obtained values are reported in Table 2.

[TABLE 2]

ALS-based estimations

Since dendrometric models were species-specific, we proceeded to map forest vegetation by classifying a L8 OLI multispectral image. We looked for two classes: broadleaves and conifers. More detailed species mapping was retained not reliable. The training set for the Minimum Distance supervised classifier was generated by *region growing* (similarity threshold equal to 0.9) starting from the position of the surveyed

151 plots centers. A total of 591 pixels were finally selected (322 for broadleaves and 269 for conifers). Classification overall accuracy was tested and resulted 90.2 %. Table 3 reports main statistics concerning Minimum Distance classification performance: Producer's and User's Class accuracy, Class Commission and Class Omission.

[TABLE 3]

Once conifers and broadleaves forest areas were mapped, the inverse dendrometric models (eq. 6) were applied specifically calibrated for both conifers "C" and broadleaves "B". In table 4 model parameters and MAE are reported.

[TABLE 4]

Models were applied at single tree level (as detected by local maxima algorithm from CHM). This made possible to compare ECDF of the explored forest estimates (see forward on).

Mean descriptive statistics about D^L_μ, H^L_μ, BA^L, T^L_{pha}, and QMD^L values for "C" and "B" classes were also computed and reported in Tab.5.

[TABLE 5]

Ground Vs ALS: testing consistency of measures

A first result from ALS dataset was tree detection and positioning. We, firstly, tested tree positions from LiDAR with the positions from ground survey. Consistency proved to be very poor (example available in Supplemental–Figure 4), and it was probably related to the low accuracy GNSS receiver used during plot surveys. Additionally, field reports indicated that only plot center was surveyed by GNSS, while tree positions inside the plots were measured using distance (m) and azimuth (degrees) from the plot center. This processes may have degraded reliability of positioning. Moreover, since plot center position was surveyed by a simple “pseudo-range” approach (C/A code measurement), the reference point (center of plot) is known to have an accuracy of 5-10 m, making final tree positioning at the ground potentially unreliable.

Consequently, only an analysis concerning aggregated measures was possible. Considering all trees falling in the sampled plots, the T_{pha} ECDFs from ground and from ALS were computed and compared (Figure 5).

[FIGURE 5]

Underestimation of trees number from ALS is probably related to the low density of the native point cloud where only trees belonging to the dominant layer of forest could be detected.

To better evaluate a possible effect of this phenomenon we also computed and compared ECDFs of H_{μ} and D_{μ} (at-plot-level aggregated measures) from both ground data and LiDAR (Figure 6).

[FIGURE 6]

ALS proved to overestimate H_{μ}, placing the majority of plot mean heights lower than 27 m; conversely, mean heights from ground surveyed plots were mostly lower than 17 m. Since D_{μ} estimation from ALS strictly depends on measured tree heights, ECDF of D_{μ} was largely different for LiDAR and ground data, showing, again, a general overestimation by ALS. ECDFs of *BA* and *QMD* from ground surveys and LiDAR were also compared. Since computations directly involve diameter values and tree numbers within plots, both *BA* and QMD from LiDAR resulted overestimated too (figure 7). BA in particular confirms that LiDAR is especially limited when recording smallest trees (i.e. smaller diameter values). In fact, overestimation of BA occurs only for its larger values (i.e. of diameter) which, given the above mentioned limitations of ALS, has to be more carefully considered.

[FIGURE 7]

According to this point of view, focusing on plot mean tree height, the difference $\Delta H_\mu = H^L_\mu - H^G_\mu$ was computed, testing its value against the expected "best" accuracy for tree height measures, i.e. intra-plot average variation of tree heights as computed from ground observations (σ^H_m = 2.86 m). We found that in 89.1 % of plots ΔH_μ exceeded σ^H_m. More complete statistics concerning all forest parameter estimations by ALS in respect of ground measures are given in table 6.

[TABLE 6]

Measures at plot level contain some apparent paradoxes, in particular concerning the relationship between ALS underestimation of tree number (T_{pha}) and overestimation of BA (for higher diameter values) and QMD. The reading key, in author's opinion, is specifically resident in the only direct measure which is expected by LiDAR, i.e. tree height. Presented data confirm that the most of estimations inconsistency is related to this native error, that, in our case study determines important overestimates of heights.

This fact should strongly alert users in adopting low density ALS datasets, making clear that an appropriate number of ground observations is however needed to avoid that such effects lead to highly distorted measures. Consequently, if ground observations (surveyed plots) are available, user has to adopt them to model *biases*, with special concerns on tree height measures from ALS.

Summarizing, observed discrepancies between LiDAR and ground measures could be related to the following two factors: a) tree density underestimation by LAS, which inevitably conditions forest parameters computations, and b) possible *biases* affecting native LiDAR point cloud.

We first explored tree density underestimation as possible reason of inconsistency. To test this assumption, we forced ground plot tree density to be equal to the LiDAR derived one (according to the strategy described in Materials and Method - *Ground vs ALS: testing consistency of measures*). This determined that new values of $H^G{}_\mu$ and $D^G{}_\mu$ were obtained ($\hat{H}^G_\mu$ and $\hat{D}^G_\mu$). Analysis was accomplished only for heights and diameters.

After reduction of ground detected trees, new MAE values resulted respectively 4.0 m for heights and 0.19 m for diameters.

Results proved that tree density is a factor conditioning consistency between LiDAR and ground tree parameters estimation. Nevertheless, once removed, residual differences suggested that some further *biases* could affect native ALS measures. Bias analysis was achieved by comparing ΔH_μ with $H^L{}_\mu$ by scatterplot. They showed a coefficient of determination R^2= 0.65 (i.e. R = 0.80), endorsing the hypothesis that a systematic error could affect LAS original data. A logarithmic regression (eq. 9) was used to model the existing *bias* (figure 8).

[FIGURE 8]

$$\varepsilon = \Delta H_{\mu} = 15.37 \cdot \ln (H_{\mu}^{L}) - 44.98 \qquad (9)$$

where ε is the correction to apply to $H^{L}{}_{\mu}$ to minimize *bias*.

Tree height *bias* model was applied at-tree level. The height of all LAS-detected trees (H_t^L) in the whole CEF were corrected (eq. 10) and new plot height mean values ($\hat{H}_{\mu}^{L}$) computed and compared with the ground surveyed ones (after tree number reduction).

$$\widehat{H_t^L} = H_t^L - \varepsilon \qquad (10)$$

New height differences $\hat{\Delta} H_{\mu} = (\hat{H}_{\mu}^{L} - \hat{H}_{\mu}^{G})$ were computed together with correspondent MAE. Statistics showed that 94.35% of heights differences, after correction, were brought within "best accuracy" ($\sigma^{H}{}_{m}$). MAE was reduced to 1.32 m. Similarly, statistics concerning new diameter differences, $\hat{\Delta} D_{\mu} = (\hat{D}_{\mu}^{L} - \hat{D}_{\mu}^{G})$, were calculated showing that 70.0 % of diameter differences, after correction, were brought within "best accuracy" (MAE^{D}). Diameter MAE was reduced from 0.19 m down to 0.08 m, greatly moving towards the "best expected accuracy" from dendrometric models.

After removing *bias* from LAS measures at-tree level, CEF was divided using a 30 m grid size graticule, computing, for each squared element, the correspondent height mean value ($\hat{H'}_{\mu}^{L}$) and tree diameter mean value ($\hat{D'}_{\mu}^{L}$) obtained considering all trees included in the element itself as detected by the Local Maxima algorithm.

ECFDs of ground- and LAS-derived (de-biased) measures were computed to test: a) if consistency ALS-derived tree heights and diameters was improved at plot level; b) if plot statistics from ground well represented the entire CEF. ECFDs are reported in figure 9.

[FIGURE 9]

Comparison demonstrated that, after *bias* removal and tree density correction, ECDFs of ground- and ALS-derived measures were more consistent. Specifically focusing on diameter values, residual inconsistency was probably due to limitation of the applied inverse dendrometric model that was calibrated without separating all tree species (calibration was at "B"/"C" class level). Given the strong improvement of LiDAR estimates of tree diameters and heights at plot level after correction, new values of $\widehat{BA}^L$ and $\widehat{QMD}^L$ were recomputed from unbiased $\widehat{H}_t^L$ and $\hat{D}_t^L$ for all the cells of the graticule covering the whole CEF. Figure 10 shows ECDFs of the new estimated parameters.

[FIGURE 10]

Figure 10 proves that BA and QMD estimates from ALS unbiased height tree measurements are more and more consistent with the ground surveyed ones. To quantify residual differences we computed MAE for both BA and QMD estimates that resulted respectively 8.5 m^2/ha and 6.0 cm.

Conclusions

This work was aimed at exploring potentialities and limits in forest parameter estimation given by low density LiDAR point clouds jointly used with medium resolution satellite data. Low density/resolution datasets are an important resource in many fields since they are often available for free by public institutions and, generally, can cover nation-wide areas. This work presents a simple and fast method to test ALS-derived forest measures and propose a model to remove error *bias* potentially affecting

LiDAR point clouds. A low-density ALS point cloud and a freely available Landsat 8 OLI image were jointly used to accomplish this task. Landsat imagery was used to map the area making possible to separate forest area were conifers prevailed from the one were broadleaves are the majority. This made possible to calibrate and apply a different dendrometric model to estimate tree diameter from height when deriving forest metrics from LidAR. The following forest metrics were estimated, at both tree an plot level, from the LAS dataset for the Cutfoot Sioux Experimental Forest (CEF) in northcentral Minnesota (USA): tree height (m) and diameter (m), basal area (m^2/ha) and QMD (cm). They were therefore tested against the available ground measures from 230 plots located in the area. A comparison at the tree level was immediately abandoned since ground measures positioning proved to be not accurate enough to recover a reliable correspondence between LAS detected and ground observed trees. All comparisons were therefore operated at plot level, by averaging local measures. Nevertheless, a not negligible inconsistency was initially found. In particular, ALS-derived measures proved to overestimate forest metrics and underestimate tree density. Accuracy of estimates was measured by MAE that resulted surprisingly high: 7.22 m, 0.21 m, 14.26 m^2/ha, 0.22 cm for H_μ, D_μ, *BA,* and *QM*D respectively; differently, tree density from LiDAR resulted greatly underestimated (ΔT_{pha} = 294.7 trees). Trees density underestimation was supposed to be related to the low density of point cloud, that determines a weak capability of LiDAR to detect trees that do not belong to the forest dominant layer. Inconsistency about forest metrics was, differently, supposed to be related to a *bias* affecting the native ALS point cloud.

The first hypothesis was initially tested by statistically removing trees of the dominated planes from the ground dataset. This determined that height and diameter MAE significantly decreased to 4.0 m and 0.19 cm respectively. Residual errors, assumed to be possibly related to a *bias* affecting the native LiDAR point cloud, were minimized by modelling b*ias* by an opportune "correction model". MAE values decreased to 1.32 m, 0.08 m, 8.5 m^2/ha, and 0.06.0 m for H_μ, D_μ, *BA,* and *QM*D, respectively. Significance of diameter and height errors was tested against the expected reference accuracy, finding that, after *bias* correction, significant errors were reduced to 5.65 % of the total for tree height, and to 30% for diameter estimates. Diameter estimate revealed to be less accurate; authors suppose that this can be mainly related to the way the diameter estimate is obtained. It is worth to remind that diameter was computed by applying a dendrometric model based on tree height estimate, whose calibration is given generally for conifers and broadleaves, with no further specification in respect of the actual tree species. Consequently, both error propagation of height estimate and model approximation are expected to affect (negatively) final accuracy of diameter estimates.

We can therefore conclude that, when working with low density LAS point clouds, tree height estimates at plot level are highly satisfying only after testing and modelling eventual error *bias*. Conversely, diameter, basal area and QMD estimates majorly suffer from uncertainty making desirable a higher point density and, probably, a better mapping of tree species (wherever possible) than the one that a remote sensing based one can generate. Further, authors retain that, in these conditions a tree level approach is not proper, and all estimates over a wide area based on low density ALS point cloud, can be reasonably given only at plot level. With these premises and under these conditions, we can however admit that, low density ALS point clouds can drive to a reasonable description and quantification of the main silvicultural metrics over wide areas, addressing more conscious management policies.

References

Aakala T., Fraver S., Palik B.J. and D'Amato A.W. 2012. Spatially random mortality in old-growth red pine forests of northern Minnesota. Can. J. For. Res.-Rev. Can. Rech. For., 42: 899-907;

Adams M.B., Loughry L. and Plaugher L. 2004. Experimental forests and ranges of the USDA Forest Service. USDA For. Serv. Gen. Technical Report, NE-321, 178;

Andersen H.E., Reutebuch S.E. and McGaughey R.J., 2006. A rigorous assessment of tree height measurements obtained using airborne lidar and conventional field methods. Canadian Journal of Remote Sensing, 32 (5): 355-366;

Baltsavias E.P., 1999. Airborne laser scanning: basic relations and formulas. ISPRS Journal of Photogrammetry & Remote Sensing, 54: 199–214;

Borgogno Mondino E., Fissore V., Lessio A. and Motta R. 2016. Are the new gridded DSM/DTMs of the Piemonte Region (Italy) proper for forestry? A fast and simple approach for a posteriori metric assessment. iForest-Biogeosciences and Forestry, 9 (6): 901-909;

Bradford J.B. and Palik B.J. 2009. A comparison of thinning methods in red pine: consequences for stand-level growth and tree diameter. Canadian Journal of Forest Research. 39: 489-496;

Buckman R.E. 1964. Effects of prescribed burning on hazel in Minnesota. Ecology, 45: 626-629;

Coveney S. 2013. Association of elevation error with surface type, vegetation class and data origin in discrete-returns airborne LiDAR, International Journal of Geographical Information Science, 27 (3): 467-483;

D'Amato A.W., Palik B.J. and Kern, C.C. 2010. Growth, yield, and structure of extended rotation Pinus resinosa stands in Minnesota, USA. Canadian Journal of Forest Research, 40: 1000-1010;

Dubayah R. and Drake J., 2000. LiDAR remote sensing for forestry applications. Journal of Forestry, 98: 44-46;

Edson C. and Wing M.G., 2011. Airborne Light Detection and Ranging (LiDAR) for individual tree stem location, height, and biomass measurements. Remote Sensing, 3: 2494-2528;

Falkowski M. J., Smith A. M. S., Hudak A. T., Gessler P. E., Vierling, L. A. and Crookston N. L. 2006. Automated estimation of individual conifer tee height and crown diameter via two-dimensional spatial wavelet analysis of lidar data. Canadian Journal of Remote Sensing, 32 (2): 153-161;

Falkowski M. J., Smith A. M. S., Gessler P. E., Hudak A. T., Vierling L. A. and Evans J. S. 2008. The influence of conifer forest canopy cover on the accuracy of two individual tree measurement algorithms using lidar data. Canadian Journal of Remote Sensing, 34 (2): S338-S350;

Fraver S. and Palik, B.J. 2012. Stand and cohort structures of old-growth Pinus resinosa-dominated forests of northern Minnesota, USA. J. Veg. Sci., 23: 249-259;

Gatziolis D. and Andersen H.- E. 2008. A guide to LIDAR data acquisition and processing for the forests of the Pacific Northwest. Gen. Technical Report.

PNW-GTR-768. Portland, OR: U.S. Department of Agriculture, Forest Service, Pacific Northwest Research Station;

Hinsley S., Hill R., Gaveau D. and Bellamy P. 2002. Quantifying woodland structure and habitat quality for birds using airborne laser scanning. Functional Ecology, 16 (6): 851- 857;

Hopkinson C., Chasmer L., Young-Pow,C. and Treitz P. 2004. Assessing forest metrics with a ground-based scanning lidar. Canadian Journal of Forest Research, 34 (3): 573-583;

Hyyppä H., Yu X., Hyyppä J., Kaartinen H., Kaasalainen S., Honkavaara E. and Rönnholm P. 2005. Factors affecting the quality of DTM generation in forested areas. ISPRS Workshop "Laser scanning 2005", Enschede, the Netherlands;

Latifi H., Fassnacht F.E., Müller J., Tharani A., Dech S. and Heurich M. 2015. Forest inventories by LiDAR data: A comparison of single tree segmentation and metric-based methods for inventories of a heterogeneous temperate forest. International Journal of Applied Earth Observation and Geoinformation 42: 162–174;

McRoberts R., Tomppo E. and Næsset E. 2010. Advances and emerging issues in national forest inventories. Scandinavian Journal of Forest Research, 25 (4): 368-381;

Means J., Acker S., Fitt B., Renslow M., Emerson L. and Hendrix C., 2000. Predicting forest stand characteristics with airborne scanning lidar. Photogrammetric Engineering and Remote Sensing, 66 (11): 1367-1371;

Montagnoli A., Fusco S., Terzagni M., Kirschbaum A., Pflugmacher D., Cohen W. B., Scippa G. S. and Chiatante D., 2015. Estimating forest aboveground biomass by low density lidar data in mixed broadleaved forests in the Italian Pre-Alps. Forest Ecosystem, 2:10;

Morsdorf F., Meier E., Kötz B., Itten K., Dobbertin M. and Allgöwer B. 2004. Lidar-based geometric reconstruction of boreal type forest stands at single tree level for forest and wildland fire management. Remote Sensing of Environment, 92 (3): 353-362;

Perala D. A. and Alban D. H. 1993. Allometric Biomass Estimators for Aspen-biased Ecosystems In The Upper Great Lakes. Res. Pap. NC-314. St. Paul, MN: U.S. Department of Agriculture, Forest Service, North Central Forest Experiment Station, 38;

Popescu S.C. 2007. Estimating biomass of individual pine trees using airborne lidar. Biomass and Bioenergy, 31 (9); 646-655;

Popescu S.C. and Zhao K. 2008. A voxel-based lidar method for estimating crown base height for deciduous and pine trees. Remote Sensing of Environment, 112 (3): 767-781;

Reitberger J., Schnörr Cl., Krzystek P. and Stilla U. 2009. 3D segmentation of single trees exploiting full waveform LIDAR data. ISPRS Journal of Photogrammetry and Remote Sensing, 64: 561-574;

Riaño D., Valladares F., Condés S. and Chuvieco E. 2004. Estimation of leaf area index and covered ground from airborne laser scanner (lidar) in two contrasting forests. Agricultural and Forest Meteorology, 124 (3-4): 269-275;

Richards J.A. 1999. Remote Sensing Digital Image Analysis. Springer-Verlag. Berlin, 240;

Saremi H., Kumar L., Stone C., Melville G. and Turner R. 2014. Sub-compartment variation in tree height, stem diameter and stocking in a Pinus radiata D. Don

Plantation examined using airborne LiDAR data. Remote Sensing, 6 (8): 7592-7609;

Schenk T., 2001. Modeling and analyzing systematic errors in airborne laser scanners, Technical Report in Photogrammetry No. 19, Ohio State University.

Suratno A., Seielstad C. and Queen L., 2009. Tree species identification in mixed coniferous forest using airborne laser scanning. Journal of Photogrammetry and Remote Sensing 64: 683-693;

VanderSchaaf C. L. 2012. Mixed-Effects Height-Diameter Models for Commercially and Ecologically Important Conifers in Minnesota. Northern Journal of Applied Forestry, 29 (1): 15-20.

Woudenberg S.W., Conkling B.L., O'Connell B.M., Lapoint E.B., Turner J.A. and Waddell K.L. 2010. The Forest Inventory and Analysis Database: Database description and user's manual version 4.0 for Phase 2., US For. Serv. Gen. Technical Report RMRS-GTR-245.

Figures

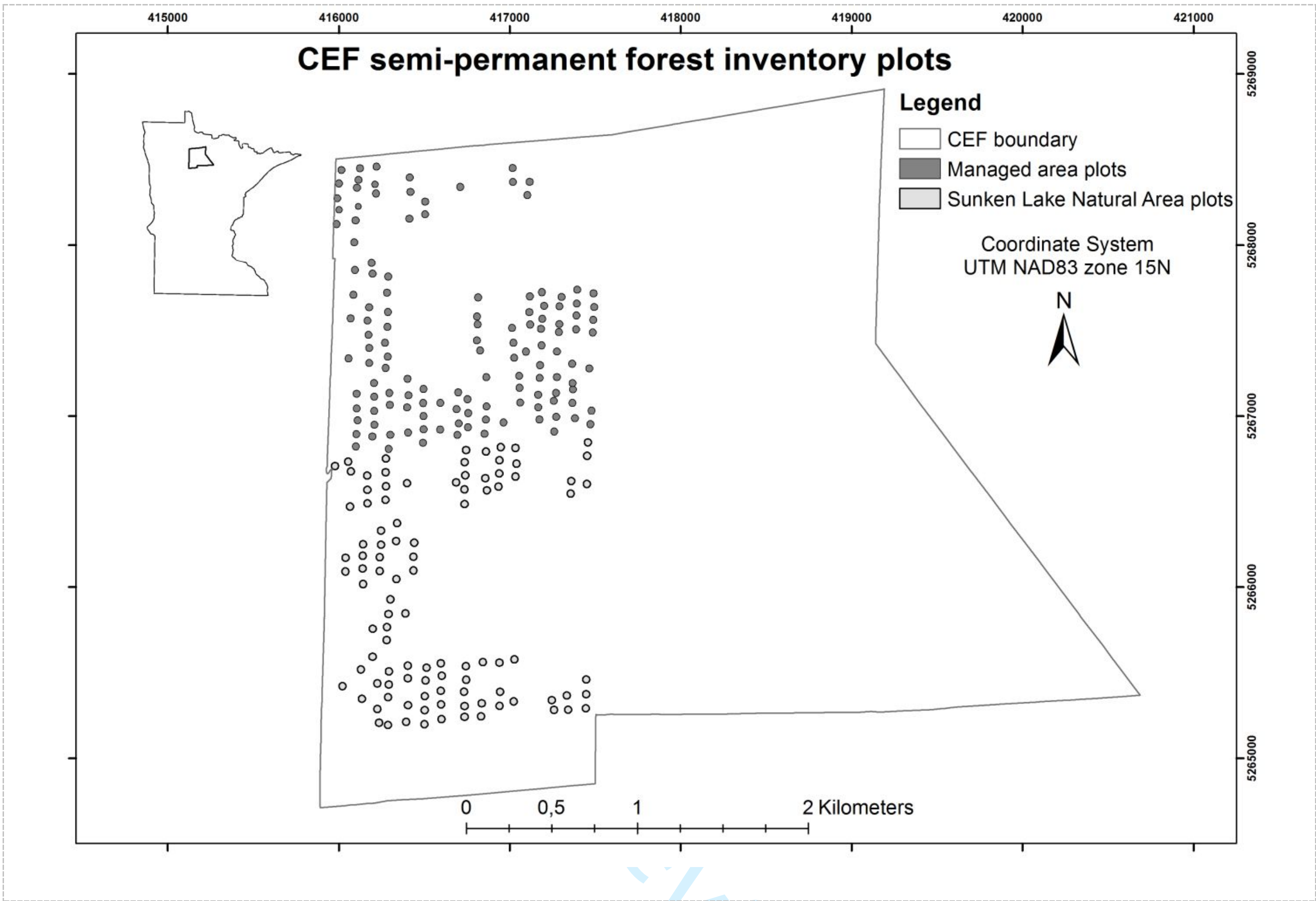

Figure 1. Map of CEF showing distribution of surveyed plots. 130 plots are located in the managed area (dark grey), 100 in the Sunken Lake Natural Area (light grey).

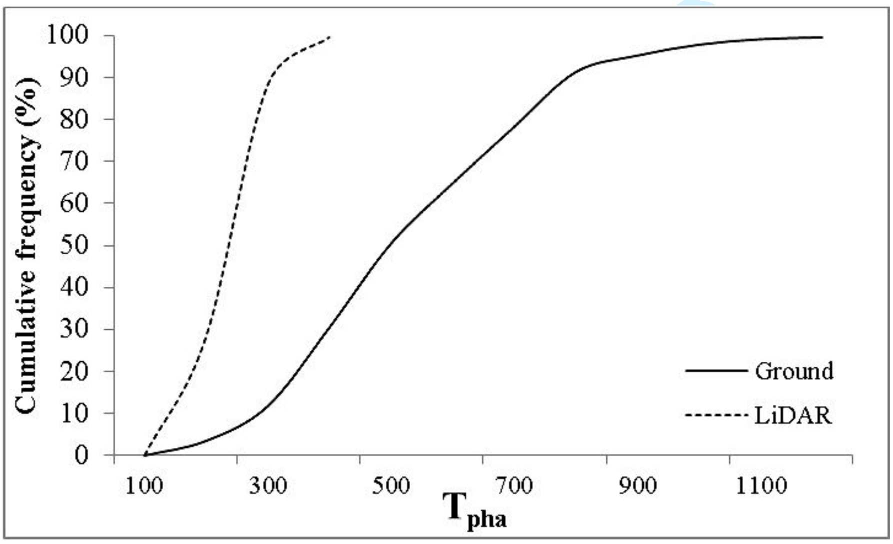

Figure 5. ECDF of ground- (solid line) and LiDAR-derived (dotted line) T_{pha}, built

considering values for all assessed plot (151).

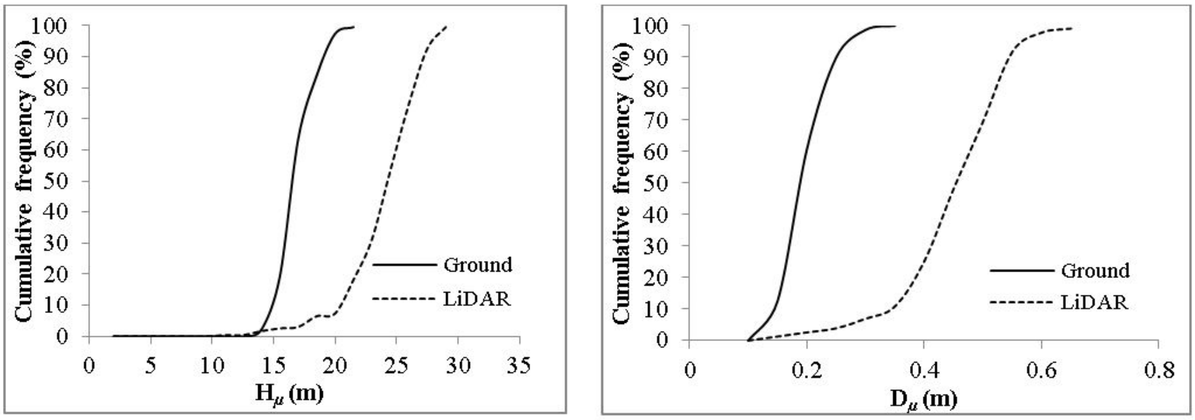

(a) *(b)*

Figure 6. ECDFs. (a) plot mean tree height and (b) plot mean tree diameter from ground (solid line) and LiDAR (dotted line).

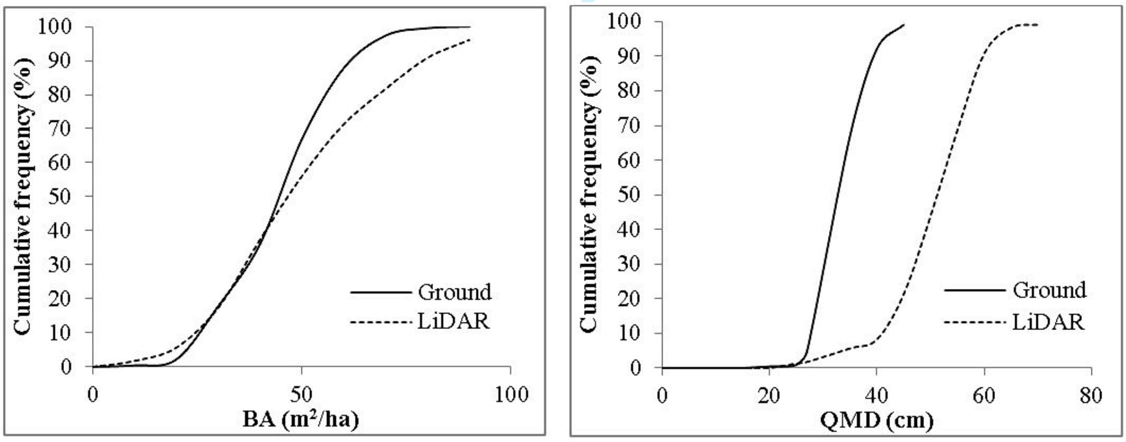

(a) *(b)*

Figure 7. ECDFs. (a) BA and (b) QMD from ground (solid line) and from LiDAR (dotted line).

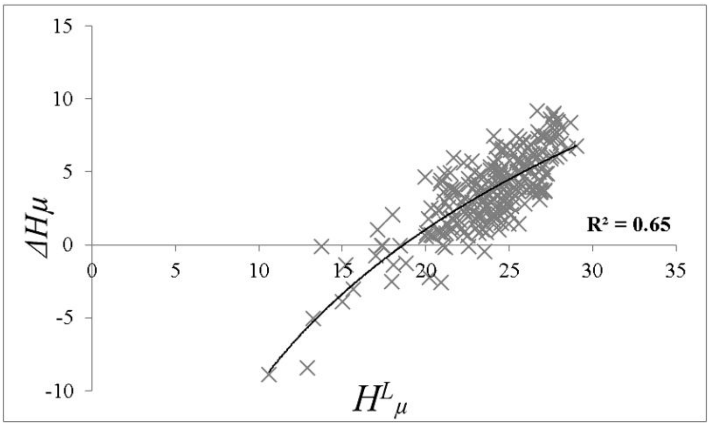

Figure 8. Bias trend modeling. The relationship linking ΔH_{μ} (height difference between ground- and LiDAR-derived measures) and $H^{L}{}_{\mu}$ (plot average tree height from LiDAR) was approximated by a logarithmic regression.

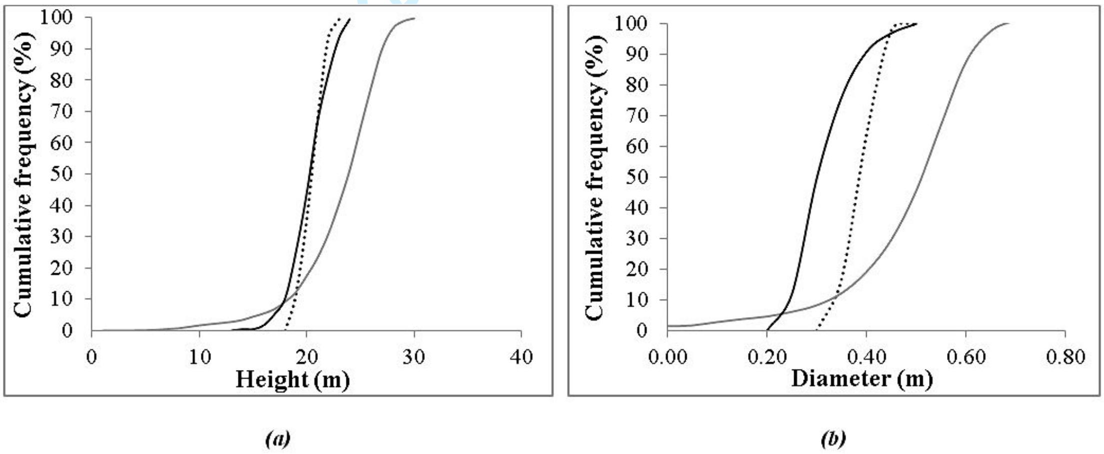

Figure 9. (a) ECDF of $\hat{H}^{G}_{\mu}$ (black solid line, ground-derived at-plot level tree height estimates after reduction), H^{L}_{μ} (grey line, LiDAR-derived at-plot level tree height estimates before bias removal) and $\hat{H}'^{L}_{\mu}$ (dotted black line, LiDAR-derived at-plot level tree height estimates after bias removal); (b) ECDF of $\hat{D}^{G}_{\mu}$ (black solid line, ground-derived at-plot level tree diameter estimates after reduction), D^{L}_{μ} (grey line, LiDAR-derived at-plot level tree diameter estimates before bias removal) and $\hat{D}'^{L}_{\mu}$ (dotted black line, LiDAR-derived at-plot level tree diameter estimates after bias removal). G= ground; L = LiDAR.

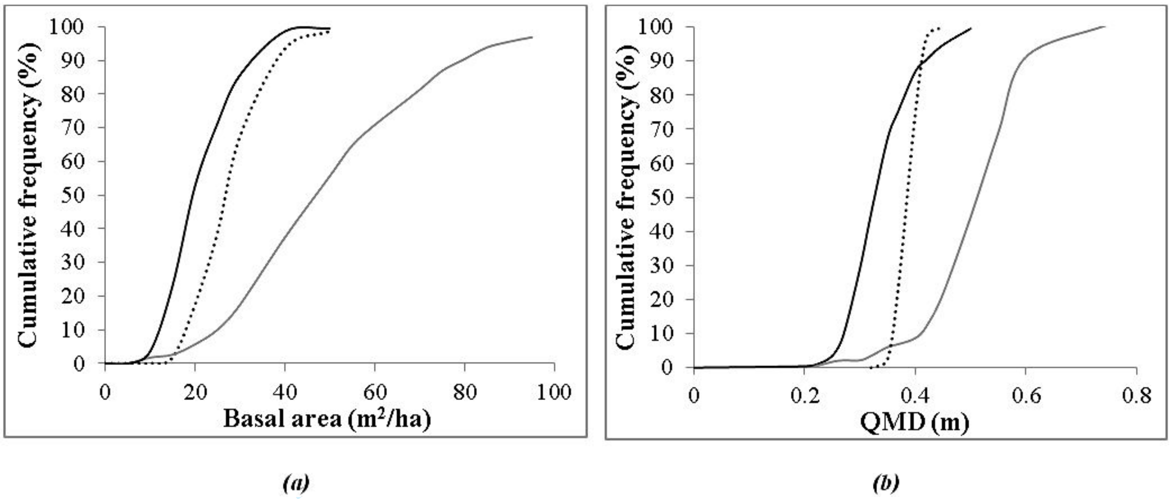

Figure 10. (a) ECDF of ground derived BA^G (black solid line), LiDAR-derived BA^L before (grey line) and $\widehat{BA}^L$ after (dotted black line) correction; (b) ECDF of field QMD^G (black solid line), LiDAR-derived QMD^L before (grey line) and $\widehat{QMD}^L$ after (dotted black line) correction. Note that ECDFs from ground estimates refer just to the plot, while ECDFs from LiDAR estimates concern all CEF (calculated at plot level considering a 30x30 grid cell). G=ground, L =LiDAR.

Table 1. Dendrometric model parameters (a_s and b_s in eq.1) estimated by OLS for the considered tree species with reference to the US FIA database. MAE^H defines the accuracy of the estimated tree height. R is the computed Pearson's coefficient for estimated and observed measures. $\sigma^H_{species}$ defines the intra-species variability of tree height estimates. In the first column it is reported, for the considered species, the macro class it was assigned to (B=Broadleaves; C=Conifers). H = tree height.

Assigned Class	*N. of trees*	*Species*	a_s	b_s	MAE^H (m)	*R*	$\sigma^H_{species}$ (m)
C	457	Balsam fir (*Abies balsamea*)	44.926	0.758	1.19	0.99	2.38
C	792	Eastern white pine (*Pinus strobus*)	39.528	0.683	2.03	0.99	3.49
C	903	Jack pine (*Pinus banksiana*)	44.925	0.730	1.48	0.98	2.84
B	411	Northern red oak (*Quercus rubra*)	30.815	0.496	1.38	0.97	3.41
B	1830	Paper birch (*Betula papyrifera*)	31.658	0.504	1.54	0.94	3.09
B	380	Quaking aspen (*Populus tremuloides*)	36.966	0.530	1.42	0.97	3.12
C	4584	Red pine (*Pinus resinosa*)	40.005	0.737	2.05	0.98	3.27

Table 2. Mean values of forest parameters at macro-class level ("B" = Broadleaves and "C" = Conifers). $\overline{\sigma_H}$; $\overline{\sigma_D}$; $\overline{\sigma_{BA}}$; $\overline{\sigma_{QMD}}$ are the average values of standard deviations of plots for each computed parameter defining its intra-class average variation. T^G_{pha} = plots mean tree density; H^G_μ = plot average tree height; D^G_μ = plot average tree diameter; BA^G= Plot total basal area; QMD^G = plot quadratic mean diameter. G = ground; L = LiDAR.

	N. of Plots	T^G_{pha} *(n tree/ha)*	H^G_μ *(m)*		D^G_μ *(m)*		BA^G *(m²/ha)*		QMD^G *(cm)*	
			Mean	$\overline{\sigma_H}$	**Mean**	$\overline{\sigma_D}$	**Mean**	$\overline{\sigma_{BA}}$	**Mean**	$\overline{\sigma_{QMD}}$
"C"	97	590.73	17.0	4.34	0.30	0.11	49.35	11.71	33.34	4.27
"B"	54	414.56	16.71	4.02	0.29	0.10	34.82	10.71	33.36	4.48

Table 3. Accuracy values of classification obtained from the available Landsat 8 OLI multispectral image..

	Conifer	***Broadleaves***
Producer Class Accuracy	89.5 %	91.4 %
User Class Accuracy	99.4 %	100.0 %
Class Commission	0.6 %	0.0 %
Class Omission	10.5 %	7.7 %

Table 4. Dendrometric model parameters (for LiDAR-derived measures, from height measures to diameter estimates) separately estimated by OLS for broadleaves and conifers. MAE^D, R and $\sigma^D_{species}$ diameter estimates statistics are reported too (D=diameter). MAE^D defines the accuracy of the estimated tree diameter from LiDAR. R is the Pearson's coefficient for estimated and observed measures. $\sigma^D_{species}$ defines the intra-species variability of tree diameter estimates.

Class	a_s	b_s	MAE^D (m)	*R*	$\sigma^D_{species}$ *(m)*
"C"	-5.156	1.388	0.045	0.985	0.006
"B"	-6.957	1.983	0.068	0.960	0.006

Table 5. Mean values of forest parameters at macro-class level ("B" = Broadleaves and "C" = Conifers) as resulting from LiDAR data. $\overline{\sigma_H}$; $\overline{\sigma_D}$; $\overline{\sigma_{BA}}$; $\overline{\sigma_{QMD}}$ are the average values of standard deviations of plots for each computed parameter defining its intra-class average variation. T^L_{pha} = plots mean tree density; H^L_μ = plot average tree height; D^L_μ = plot average tree diameter; BA^L= Plot total basal area; QMD^L = plot quadratic mean diameter.

Area	T^L_{pha} *(n.tree/ha)*	H^L_μ *(m)*		D^L_μ *(m)*		BA^L *(m²/ha)*		QMD^L *(cm)*	
		Mean	$\overline{\sigma_H}$	**Mean**	$\overline{\sigma_D}$	**Mean**	$\overline{\sigma_{BA}}$	**Mean**	$\overline{\sigma_{QMD}}$
"C"	246.89	24.73	2.20	0.51	0.06	53.22	19.76	52.0	6.58
"B"	216.47	22.13	2.98	0.47	0.12	43.82	24.45	48.97	10.78

Table 6. Percentages of plots over/under –estimating H_{μ}, D_{μ}, BA, T_{pha} and QMD from LiDAR in respect of the ground surveyed ones.

	Overestimation by LiDAR	***Underestimation by LiDAR***	***MAE***
	Plots (%)		
T_{pha} (trees num.)	3.1	96.9	294.73
H_{μ} (m)	96.5	3.5	7.22
D_{μ} (m)	97.0	3.0	0.21
BA (m^2/ha)	54.7	45.2	14.26
QMD (cm)	95.6	4.75	0.22

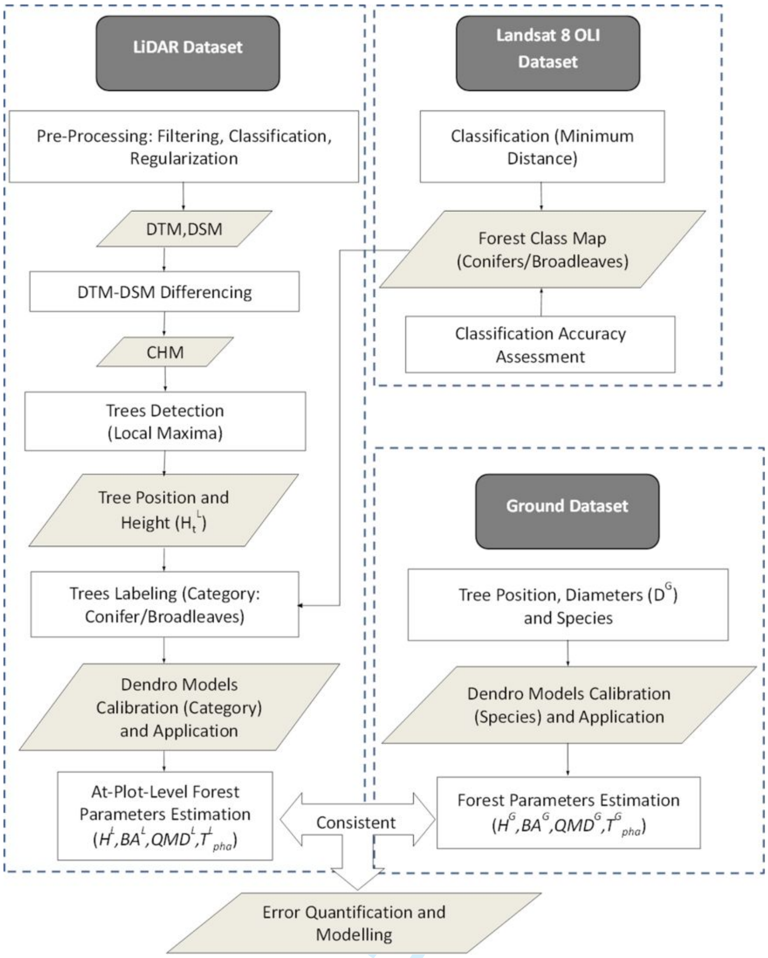

Figure 2. Flowchart showing LiDAR and ground data main processing steps for forest parameters computation.

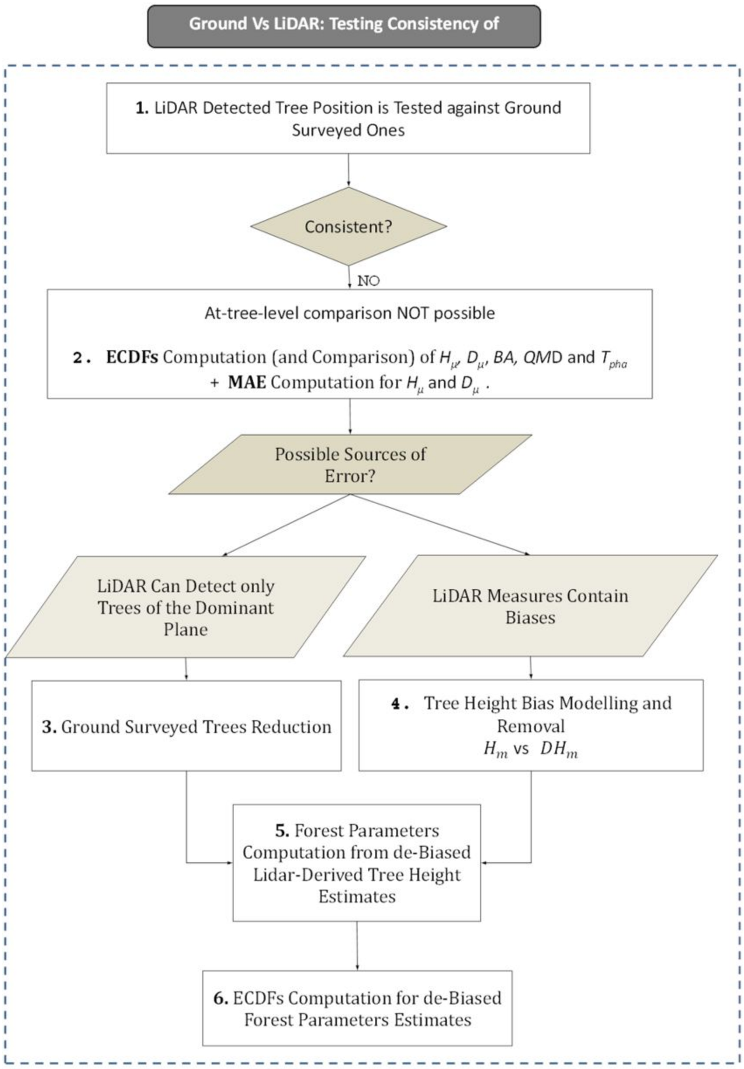

Figure 3. Flowchart showing processing steps of accuracy assessment aimed at improving consistency between LAS and ground derived forest measures in the Cutfoot Sioux Experimental Forest.

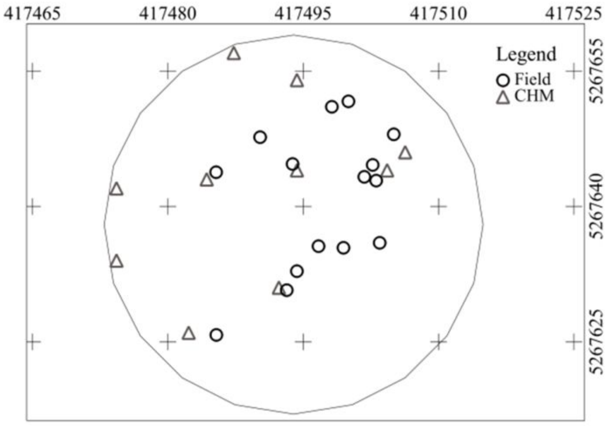

Figure 4. Example plot (n. 2019) showing spatial inconsistency between tree positions from ground survey (black spots) and LiDAR detection by Local Maxima algorithm (grey triangles).